Article

Discovery and Development of SPR519 as a Potent, Selective and Orally Bioavailable Inhibitor of PI3Kalpha and mTOR Kinases for the Treatment of Solid Tumours

Dinesh Mahajan, Somdutta Sen, Bilash Kuila, Amit Sharma, Reena Arora, Milind Sagar, Amal Ray Mahapatra, Lalita Babasaheb Gawade, and Sundeep Dugar

J. Med. Chem., **Just Accepted Manuscript** • DOI: 10.1021/acs.jmedchem.0c01061 • Publication Date (Web): 08 Sep 2020

Discovery and Development of SPR519 as a Potent, Selective and Orally Bioavailable Inhibitor of PI3Kα and mTOR Kinases for the Treatment of Solid Tumors

Dinesh Mahajan,[1]*† Somdutta Sen,[1] Bilash Kuila,[1] Amit Sharma,[1] Reena Arora,[1] Milind Sagar,[1] Amal Ray Mahapatra,[1] Lalita Babasaheb Gawade,[1] Sundeep Dugar,[2]*

[1]Sphaera Pharma Pvt. Ltd., Plot 32, Sec 5, IMT Manesar, Haryana 122051, India.

[2]Sphaera Pharma Pte. Ltd., 038988, Singapore.

KEYWORDS PI3K, mTOR, dual inhibitor, cancer, triazine

ABSTRACT: Herein we report, the identification and pre-clinical profile of a lead compound **10**, (**SPR519)** as an equally potent dual inhibitor of PI3Kα and mTOR kinases. **SPR519** exhibits an EC_{50} of low sub micro molar range among various tested cancer cell lines such as A2780 (0.23 μM), PC3 (0.48 μM), and SKOV3 (0.50 μM) respectively. When administrated orally, it shows a considerably high plasma exposure (AUC: 26,858 nM/h at 1 mg/Kg) in mice. Moreover, it is found to be safe in animals with a dose of 30 mg/Kg BID for 12 days in dose tolerance study. **SPR519** did not show any CYP or hERG liability. The identified lead demonstrates significant efficacy and bioavailability in ovarian and colon cancer xenograft models when evaluated for dose-ranging efficacy studies, at a dose as low as 2.5 mg/Kg.

INTRODUCTION

Phosphatidyinsoitol-3-kinases (PI3Ks) play a key role in cell proliferation, growth and survival.[1-2] Dysregulated activity of PI3Ks has been implicated in poor prognosis and survival in patients with various solid as well as liquid tumors.[3] There are four classes of PI3Ks reported in literature.[4] Ambiguity over the involvement and role of individual PI3K isoforms of class I PI3Ks in various types of tumors leads to an argument on isoform specific over pan PI3K inhibitors for therapeutic efficacy against cancer.[5] However, literature suggests a prominent role of PI3K α and PI3Kδ isoforms of class I PI3Ks in human cancer biology. The dysregulated activation of PI3K α or other isoforms of class I PI3K group and its downstream effectors including AKT and mTOR have been linked to tumor initiation and maintenance.[6] So, an effective inhibitor of the PI3K/AKT/mTOR pathway could both prevent cancer cell proliferation and induce programmed cell death (apoptosis). Significant efforts have been made in drug discovery to develop therapeutic interventions for cancer by inhibiting the functional roles of PI3K, AKT, or mTOR in this signaling pathway.[6-7] The selective inhibition of mTOR kinase faces a challenge of drug resistance due to over activation of oncogene PI3Kα by a feedback mechanism involving S6 kinase.[8] Recent literature reports suggest that single molecule based dual inhibitors of PI3K/mTOR may have better therapeutic advantages over stand-alone PI3K or mTOR inhibitors, but this certainly requires clinical validation.[9]

Stocks *et al.* discussed and described different structure classes of PI3K inhibitors and their design strategies from medicinal chemistry prospectus in an elegantly collated review.[10] There are quite a few PI3Kα inhibitors known in literature based on morpholine substituted triazine core. Few pharmacologically well characterized advance leads in this structure class are mentioned in Figure 1. Compound **ZSTK474** was the first published clinical lead based on morpholine substituted triazine core having pan PI3 kinase activity.[11] **PKI-587** was a second inhibitor disclosed in this class possessing PI3K/mTOR dual activity.[12] **PKI-587** is an experimental drug under phase 2 evaluation at present. **PQR309** is a PI3K/mTOR dual inhibitor in phase 2 trials.[13] Wymann *et al.* has published an ingenious SAR study to understand PI3K/mTOR differential activity leading to discovery of **PQR309** and other follow-up analogues *i.e.,* **PQR514** and **PQR530**.[13-15] It is interesting to see how minor structural changes can lead to improve in potency as well as mTOR activity. In all these reported inhibitors, oxygen atom of morpholine found to have a critical hydrogen bond interaction with NH of the amino acid residue Val851 (PI3Kα) and Val2240 (mTOR) in the hinge region.[11-16] The aryl group of these reported inhibitors is understood to occupy affinity pocket of ATP binding site of the PI3Kα. The presence of two morpholine units put these reported leads under a common genus.

In our ongoing endeavor for the development of cancer therapies based on the targeted inhibition/modulation of PI3K/AKT/mTOR signaling pathway, we reported the discovery of an early lead compound **26**.[17] Compound **26** was found to be an orally bioavailable, well-tolerated potent inhibitor of PI3K α. Herein, we report further optimization and development studies around this initial hit leading to discovery of a more potent as well as efficacious analogue compound **10**, an equipotent dual inhibitor of PI3K α and mTOR proteins (Figure 1).

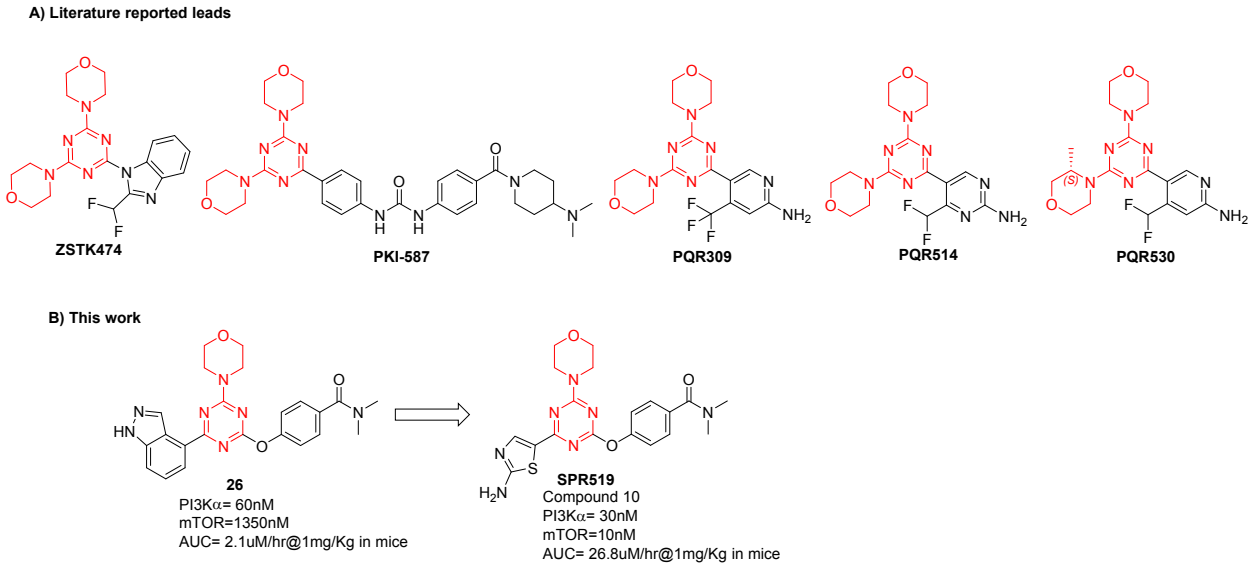

Figure 1: PI3Kα inhibitors reported in literature based on morpholine substituted triazine scaffold.

RESULTS AND DISCUSSION

In the course of our efforts towards development of a dual PI3K/mTOR inhibitor, we designed and synthesized new analogues around **26** and evaluated them for PI3Kα enzyme inhibitory activity as well as cellular potency against human ovarian cancer cell line (A2780). The new analogues were designed with an aim to enhance *in vitro* therapeutic potency. The variations on indazole heterocycle was selected as a preferred alteration on initial lead **26** based on the previously reported SAR and understanding by us[17-18] and others,[19-20] where it is understood to be a critical pharmacophore for potency. The new series of compounds were designed and synthesized (Table 1), as replacements of indazole. All new analogues **1-12** were synthesized using Scheme 1 as reported before.[21] To facilitate rapid analogue synthesis, we utilized **13** as a late stage key intermediate for Suzuki coupling reactions with various aryl boronates, exploiting $Pd(PPh_3)_4$ as catalyst in biphasic reaction conditions. The desired core **13** was synthesized in multi gram scale exploiting nucleophilic addition of morpholine followed by addition of 4-hydroxy benzamide on commercially available cyanuric chloride.[21]

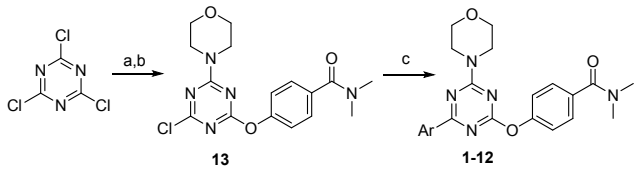

Scheme 1: Synthesis of compounds **1-12** for SAR study. Reagents and conditions: (a) Morpholine (1 equiv), anhyd. THF, DIPEA (1 equiv.), 0 °C, 2 h, 69%; (b) 4-Hydroxy benzamide, anhyd. DMF, K_2CO_3 (2.5 equiv.), 18-Crown-6 (catalytic), 60 °C, 4 h, 88%; (c) Aryl borate (1.5 equiv.), $Pd(PPh_3)_4$ (0.1 equiv.), Na_2CO_3 (3 equiv.), DME: water (4:1), 100 °C or microwave irradiation, 16-20 h, HCl in dioxane (4N), RT, 30-60 min, 60-85%.

All new compounds synthesized using this synthetic route were evaluated for their *in vitro* PI3Kα inhibition activity. The PI3Kα enzyme inhibitory activity of the new compounds was determined using a Homogeneous Time Resolved Fluorescence (HTRF) assay. The percentage of inhibition was calculated and plotted against the concentration of the inhibitor to calculate the IC_{50}. The newly synthesized analogues in this series were also screened for their cellular potency. The cellular potency was determined by the MTT assay using human ovarian cancer cell line (A2780).

Compound **1** was found to be the most potent analogue with an IC_{50} of 10 nM against PI3Kα and EC_{50} of 0.09 μM in A2780 cell line. Compared to **26**, compound **1** exhibited 6-fold higher potency (both for enzymatic as well as cellular activity) and was further considered for pharmacokinetic study. Disappointingly, the pharmacokinetic analysis indicated no plasma exposure for compound **1** when administrated orally to a group of mice at a dose of 10 mg/Kg. The absence of plasma levels is probably related to the potentially rapid Phase II conjugation and clearance associated with the phenolic group of **1**. Interestingly, none of other analogues synthesized had better affinity for PI3Kα protein except **10**. But compounds **2**, **3**, and **8** (Table 1) showed improved or equal cellular potency compared to **26**. Replacement of indazole with similar bicyclic moieties (*i.e.,* compounds **7**, **8**, and **9**) provided interesting insights. The change from indazole (**26**) to indole (**7**) resulted in a significant drop in potency, which regained significantly in the azaindole analog (**8**; IC_{50} = 0.08 μM). This possibly suggested the involvement of pKa of the NH of the hetroaryl, in this series of compounds. However, replacement with the benzotriazole (**9**) resulted in a total loss of potency (IC_{50} = > 10 μM). Replacement of indazole with amino-pyridine (**3**; IC_{50} = 0.21 μM) or amino-pyrimidine (**2**; IC_{50} = 0.27 μM) led to a 3 to 4-fold loss in kinase activity. Introduction of steric constraints in compound **3**, through methyl group on the pyridine ring (compound **4**, **5** and **6** compared to compound **3**) found to have dramatic effect on IC_{50} value. Methyl substitution was found to be more tolerable at 5-position of pyridine ring (*i.e.* compound **4**). Compound **10** with a five member heterocycle as a new replacement of indazole led to 2-fold increase in activity. Here again, an additional substitution of methyl on this five-member heterocycle resulting in compound **11** proved detrimental for

ligand protein interaction. Interestingly, but with no obvious explanation available, compound **2**, **3**,

Table 1: Medicinal chemistry optimization and SAR around initial hit **26**.

Compound Number	*Ar*	*PI3Kα* *$^{*}IC_{50}$ (μM)*	*Cell line A2780* *$^{*}EC_{50}$ (μM)*
26	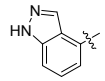	0.06	0.52
1	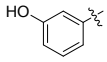	0.01	0.09
2	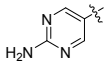	0.27	0.56
3	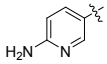	0.21	0.20
4	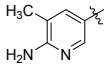	0.46	1.5
5	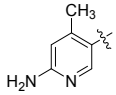	>10	>10
6	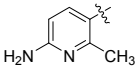	3.40	>10
7	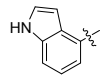	0.56	0.90
8	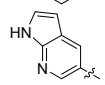	0.08	0.37
9	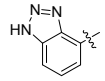	>10	>10
10	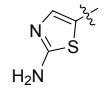	0.03	0.23
11	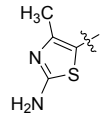	0.14	1.1
12	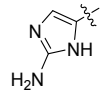	0.90	2.36
GDC0940	-	0.04	0.29

*All the experiments were done in triplicates. The coefficient of variation (CV %) was found to be <10% for IC_{50} and <5% for EC_{50}.

and **8** demonstrated comparable or higher cellular potency with respect to **26** even though they have lower IC_{50}. A possible explanation for this could be enhanced cellular permeability of these compounds or perhaps involvement of an additional complementary target leading to enhanced cellular potency. We envisaged that enhanced cellular permeability, however, might be less likely to be the reason for this increased potency as these compounds are structurally similar. We next investigated the possibility of the involvement of a complementary target. It is reported that PI3Kα and mTOR share a high degree of sequence homology. Keeping this understanding in mind we screened some selected molecules for their mTOR binding affinities along with PI3Kα as well as cellular potency. Two different cancer cell lines were used to evaluate their EC_{50}. The results are tabulated in table 2. As is evident from the data, these compounds demonstrated a good affinity for mTOR along with PI3Kα. The compounds **26**, **2**, and **8** showed higher affinity for PI3Kα (0.06 μM, 0.27 μM and 0.08 μM) compared to mTOR (1.35 μM, 0.96 μM and 0.22 μM) while compounds **4** and **10** showed equal affinities for PI3K and mTOR proteins. The new compounds **2**, **3**, **8**, and **10** are also found to be more potent in prostate cancer cell line (PC3) as well as ovarian cancer cells (A2780) compared to initial hit **26**.

Table 2: Potency evaluation of identified leads.

	$^{*}IC_{50}$ and $^{*}EC_{50}$ (μM)					
Compound Number	Ar	p110 α	mTOR	PC3	SKOV3	logP/tPSA[#]
26		0.06	1.35	1.97	0.52	3.78/103.5
2		0.27	0.96	0.80	0.22	2.4/129.8
3		0.21	0.20	0.28	0.21	3.21/117.5
8		0.08	0.22	0.30	0.37	3.58/103.5
10		0.03	0.01	0.48	0.50	3.6/117.5

* All the experiments were done in triplicates. The coefficient of variation (CV %) was found to be <10% for IC_{50} and <5% for EC_{50}. [#] Values are calculated using ChemOffice 2015.

Based on the dual activity of compounds **3**, **8**, and **10** and high cellular efficacy, these three leads were further evaluated for their *in vitro* metabolic stability using human liver microsome (HLM), dog-liver microsome (DLM), and mouse liver microsomes (MLM). The three leads were incubated individually, with liver microsomes of three different species for 2 h. The concentration of the parent compound was monitored by HPLC at four-time points. All three leads (**3**, **8**, and **10**) showed a high level of microsomal stability, particularly in HLM (Table 3), just like original lead **26**. These three molecules were also evaluated for oral bioavailability in mice. The results are summarized in table 3. All new compounds demonstrated higher plasma exposure than the original lead **26** when administrated orally to a group of mice (3 mg/Kg). Compound **10** showed considerably better pharmacokinetic (PK) profile compared to others leads (AUC >32 μM.h). This study concluded that replacement of indazole (**26**) with 2-aminothiazole (**10**) provided higher potency for mTOR and higher plasma exposure.

The lead compounds **3**, **8**, and **10** were further evaluated for possible hERG liability. Compounds were screened for hERG activity using the HERG-lite assay from Chantest Corporation. The objective of the study was to estimate the *in vitro* effects of these leads on surface expression of the hERG potassium channel. Both wild type (WT) and the single-point mutant (SM) channel G601S were

examined. Predicted hERG liability was indicated as channel block and/or trafficking inhibition. While none of the lead showed trafficking inhibition, but all of these demonstrated channel blocking. On the basis of the hERG lite assay data, the IC_{50} of the hERG liability was predicted by the patch-clamp method. The anticipated hERG liability of **3** was found to be >1 μ M, while those of compound **8** and **10** were >10 μ M (Table 4), which was very encouraging.

All three leads showed no or minimal inhibitions for activity against CYP3A4, CYP2C19, and CYP2D6 at 10 μM concentration, as mentioned in table 4. Based on its potency and DMPK profile, compound **10** was selected for further evaluation. To evaluate off-target selectivity, compound **10** was screened for its binding affinity against a panel of kinases. A panel of 23 kinases was selected based on their close sequence homology with PI3Kα and/or mTOR protein. The lead **10** was screened at a single concentration of 1 μM across this panel. The results are mentioned in table 5. This screening demonstrated that the lead **10** has similar inhibitory activity against PI3Kδ along with PI3Kα and mTOR kinases. With encouraging level of selectivity across a limited panel of kinases, it was planned to profile **10** *in vivo* in mice to evaluate pharmacological parameters and optimum dosing regimen for efficacy studies. We performed a dose-ranging in pharmacokinetics and multi-day repeat dose toxicity studies to understand dose linearity and tolerable dose in a rodent model.

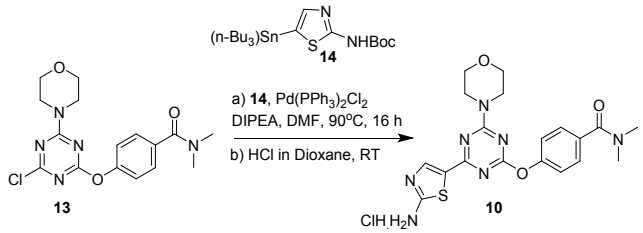

Scheme 2: Multigram synthesis of **10**

Table 3: Metabolic stability and pharmacokinetic analysis of leads.

		*Metabolic stability**			*Mouse Pharmacokinetic***			
Compound Number	Ar	DLM	MLM	HLM	AUC (nM/h)	C_{max} (nM)	T_{max} (h)	$t_{1/2}$ (h)
26	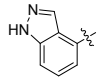	83	45	100	5246	1243	1.0	4.9
3	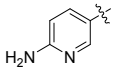	93	102	93	10940	2010	1.4	2.7
8		77	68	92	16770	3076	1.0	2.8
10		105	103	98	32146	6903	1.5	2.7

*@10 μM: %remaining after 2 h; ** n=3/group; PO @ 3mpk; C_{max}: maximal concentration, T_{max}: time of maximal, concentration in hours; $t_{1/2}$: half-life elimination; AUC: area under the curve.

Table 4: Off-target screening of the leads.

		CYP inhibition IC_{50} (μM)			*hERG binding*		
Compound Number	Ar	CYP 3A4	CYP 2C19	CYP 2D6	Channel Blocking	Trafficking Inhibition	Predicted IC_{50} (μM)
3	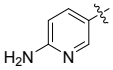	>10	>10	>10	Yes	No	>1.0
8		>10	>10	>10	Yes	No	>10.0
10		>10	>10	>10	Yes	No	>10.0

Table 5: Screening of lead **10** across a small panel of human kinases at 1 μM concentration.

Sr No	*Kinase*	*% inhibition*	*Sr No*	*Kinase*	*% inhibition*
1	AKT1	-1	13	PDK1	-1
2	AKT2	0	14	PI3Kα	86
3	AKT3	-1	15	PI3Kβ	42
4	ERBB2	-1	16	PI3Kδ	88
5	FLT3	9	17	PI4Kβ	-3
6	GSK3B	-1	18	PRKCZ	0
7	IKBKB	-3	19	SPHK1	-1
8	IKBKE	-1	20	TIE2	1
9	MEK1	0	21	TRKA	3
10	MEK2 (MAP2K2)	1	22	CDK7	-10
11	P70S6K1 (RPS6KB1)	-1	23	mTOR	89
12	RPS6KB2	-3			

In dose-ranging pharmacokinetic study, compound **10** was evaluated for various parameters at three incremental oral doses of 1, 3, and 10 mg/Kg in Swiss mice (Table 6). A dose-dependent increase in plasma exposure (AUC) was observed without any significant change in T_{max} and $T_{1/2}$ at three different doses. However, C_{max} did not show any dose linearity at three tested doses.

Table 6: Detailed pharmacokinetic analysis of **10**

		Swiss Mouse PK (Oral)			
Compound	dose	AUC (nM/h)	C_{max} (nM)	T_{max} (h)	$T_{1/2}$ (h)
10	1 mg/Kg	26858	5014	1.33	2.66
	3 mg/Kg	32146	6903	1.50	2.74
	10 mg/Kg	76365	12558	1.67	2.52

C_{max}: maximal concentration, T_{max}: time of maximal, concentration in hours; $t_{1/2}$: half-life elimination; AUC: area under the curve

For the planned dose tolerance and efficacy studies in rodents, multi-gram quantity of compound **10** was required. Attempts to get gram-scale synthesis of **10** using Scheme 1 through Suzuki coupling of corresponding boronic acid was not efficient due to practical limitations involving poor yields and/or need of a microwave reactor. Most of the gram-scale attempts for Suzuki coupling of boronic acid led to undesired dehalogenation of **13** as a major product. To solve this problem, a Stille coupling based synthesis was developed as presented in Scheme 2. An organo-tin reagent (**14**) was synthesized in lab.[21] The core **13** was subjected to a Stille coupling with **14**, followed by a treatment with a premixed solution of HCl in dioxane lead to formation of compound **10** in high yield.[21] This reaction was performed on 10 gm scale to afford sufficient amount of **10** to support all necessary animal experiments.

A repeat dose tolerance study was performed at two different doses of 10 mg/Kg and 30 mg/Kg, twice daily (BID), oral for 5 days, and 12 days respectively. For this, three study groups (two doses and one vehicle control group) of mice were selected. All three groups were observed daily for bodyweight loss as well as other vital clinical signs such as loss of appetite, body coat, eyes, feces, and general body conditions. In the 10 mg/Kg group after 5 days of treatment, no significant average weight loss was observed compared to vehicle control. There was no change in clinical or vital signs seen in the 10 mg/Kg BID dosing group. However, slight piloerection was observed on the 9th day in 30 mg/Kg BID dosing arm. A tissue distribution analysis was done in Swiss female mice. Mice were dosed orally at 30 mg/Kg, twice a day for five consecutive days to determine the drug accumulation and distribution in different vital organs. After 30 mg/Kg BID/five day dosing, animals were sacrificed, and their liver, kidney, lung, uterus, and brain were extracted and observed for any physical color change as well as test drug concentration. No change in physical morphology or discoloration was observed in these vital organs except very faint color change in the liver. The LCMS analysis of the homogenized extracted organs showed maximum drug concentration (Figure 2) in kidneys (160 ng/g) followed by liver (85 ng/g), lungs (50 ng/g), and uterus (10 ng/g). No significant amount of test drug was observed in the brain of the animals.

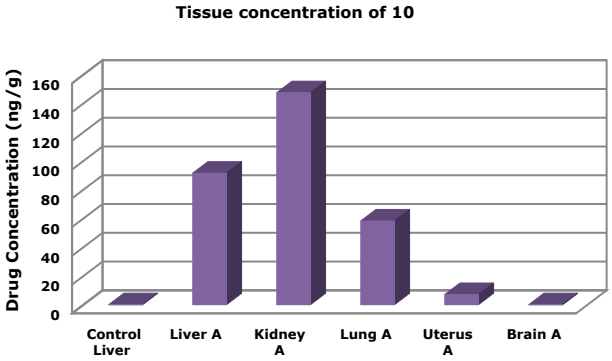

Figure 2: Distribution/accumulation of 10 in tissues after 5 days repeat dosing with 30 mg/Kg BID oral in Swiss female mice.

Based on the encouraging *in vitro* and *in vivo* profile of the lead **10**, we planned to determine *in vivo* efficacy against two different solid tumors. An efficacy study in two individual xenograft models with CD1 nude female mice was performed using SKOV-3 (ovarian cancer) and HCT116 (colon cancer) cells. In each xenograft study, tumor was allowed to grow and sustain for a few days to a specific pre-defined tumor volume before start of treatment with compound **10**. Animals were randomized and divided in different groups (3 or 4 doses and one control) with five animals per group. The average body weight of animals and tumor volume was within the same range across all groups. The three dosing groups in the case of SKOV-3 model were treated with three different incremental oral doses of **10** (2.5, 5, and 10 mg/Kg; once-a-day) for 27 days. Similarly, four dosing groups of HCT116 model were treated with four different doses of **10** (2.5, 5, 10, and 20 mg/Kg once-a-day) for 21 days. Tumor volume was determined every third day to monitor the study progress for each dosing group (Figures 3 and 4). It was encouraging to see a considerable inhibition of tumor growth in two different tumors after first 3 days at dose as low as 2.5 mg/Kg. This reduction in tumor volume was dose-dependent, with all treated animals responding in the treated groups compared to the untreated group. The study was terminated on day 28 for SKOV-3 and day 22 in the case of HCT116 due to animal ethics reasons as untreated arms in two cases had to be sacrificed because of large tumor volume. It was exciting to see a considerable inhibition in tumor growth in both studies within the initial 3 days at a dose as low as 2.5 mg/Kg to 20 mg/Kg QD, which was consistent with the progress of the study.

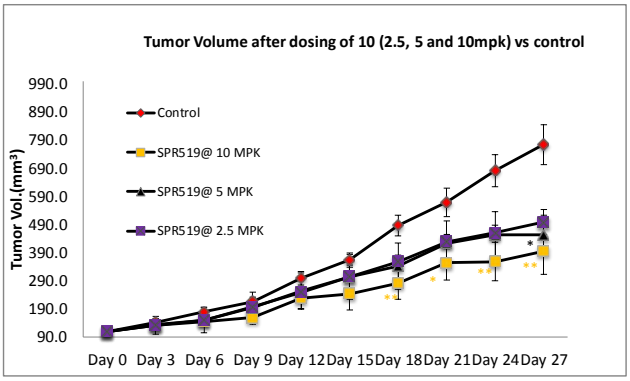

Figure 3: Tumor growth inhibition study after oral dosing of 10 in mice xenograft model, inoculated with SKOV-3 cell line**.** The tumor volume was determined at each time point. Statistics analysis was done using two-way ANOVA with Dunnett's multiple comparisons test: *p<0.05; **p<0.01; n=5

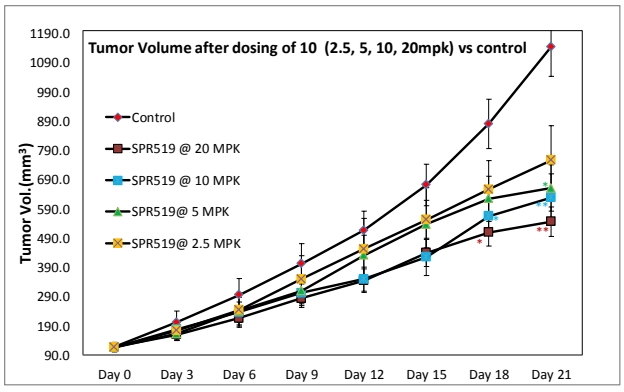

Figure 4: Tumor growth inhibition study after oral dosing of **10** in mice xenograft model, inoculated with colon cancer (HCT116). The tumor volume was determined at each time point. Statistics analysis was done using two-way ANOVA with Dunnett's multiple comparisons test: *p<0.05; **p<0.01; n=5

CONCLUSION

In conclusion, our efforts towards development of drug like molecules for the treatment of solid tumor led to the identification of a drug lead **10** (SPR519). **SPR519** is a potent inhibitor of PI3Kα and mTOR kinases. The identified lead was evaluated *in vivo* and found to be orally bioavailable, and well-tolerated up to a high dose of 30 mg/Kg. **SPR519** was found to be efficacious in animal models of ovarian and colon cancer. It was encouraging to see noticeable efficacy in ovarian cancer xenograft at lower oral dose (2.5 mg/Kg). Further pre-clinical investigations are in progress to develop **SPR519** as a candidate for investigational new drug studies.

EXPERIMENTAL SECTION

General information: Unless otherwise noted, commercial available materials were used without further purification. Air sensitive reactions were carried out under argon atmosphere. Anhydrous solvents were obtained from Sigma Aldrich, Merck. Thin layer chromatography (TLC) was carried out using 0.2 mm Kieselgel F254 (Merck) silica plates and compounds viewed under an ultraviolet lamp. NMR spectra were recorded on a Bruker 300 MHz spectrometer operating at 300 MHz for ^{1}H and 75 MHz for ^{13}C. Chemical shifts (δ) are quoted in parts per million (ppm) relative to internal solvent reference ($CDCl_3$ δ = 7.26 for ^{1}H NMR and δ = 77.0 for ^{13}C NMR and DMSO-d_6 δ = 2.50 for ^{1}H NMR and δ = 39.9 for ^{13}C NMR). Coupling constants are given in Hz. Data is reported as followed: chemical shift, multiplicity (s = singlet, bs = broad singlet, d = doublet, t = triplet, dd = double doublet, dt = double triplet, m = multiplet), coupling constants (Hz), and integration. Purity of all new compounds was > 95% and confirmed using high performance liquid (HPLC) chromatography. The actual purity of individual compounds is mentioned in experimental detail. The detailed HPLC method used for purity determination is provided below. Mass spectra were recorded in ESI mode on an Agilent 6120 Quadrupole LC/MS instrument. HRMS spectra were recorded on Agilent HRMS-6540-UHD machine at IIIM Jammu, INDIA. Authors confirm that all animal experiments performed in the manuscript were conducted in compliance with institutional guidelines following ethical guidelines and necessary approvals.

HPLC method for chemical purity determination: The chemical purity of the final compounds and/or intermediates were characterized by high performance liquid chromatography (HPLC) using a Waters Millenium chromatography system with a 2695 Separation Module (Milford, MA). The analytical columns used for this analysis was Gemini C-8 4.6 x 150 mm 5 micron with flow rate 1 mL/min of mobile phase consist of a mixture of water and acetonitrile. A gradient elution was used, typically starting with 5% acetonitrile/ 95% water contained 0.1% trifluoroacetic acid (TFA) with a progression to 100% acetonitrile over a period of 20 min. Compounds were detected by ultraviolet light (UV) absorption at either 220 or 240 nm. HPLC grade solvents were procured from Merck and Fisher Scientific.

Synthesis of compound 26, 13 and 14: Compounds was synthesized as per previously reported procedures.[17,21]

General procedure for synthesis of compounds 1-12:[21] To a solution of compound **13** (1 mmol) in DME: H_2O (4:1; 10 mL) was added corresponding aryl boronic acid or boronate ester (1.5 mmol) and Na_2CO_3 (3 mmol). Degassing of the reaction was done for 5 min (using nitrogen and vacuum in repeated cycles) followed by addition of $Pd(PPh_3)_4$ (0.1 mmol) under inert atmosphere. The reaction mixture was heated at 100-110 °C for 16-20 h. Alternatively, reaction can be performed using microwave irradiation for 1-2 h. The progress of reaction was monitored using TLC (1-5% MeOH in DCM). After completion, excess of solvent was removed under vacuum, the reaction mass was diluted with water and extracted with of DCM (3 x 100 mL). The organic layer was separated, dried over Na_2SO_4, filtered, and concentrated under reduced pressure to obtain crude product. Further purification was done by silica gel chromatography to obtain pure product. In case of compounds **3**, **8**, **10** and **12**, since *N*-Boc protected aryl boronate esters were used, obtained products were further treated with HCl in dioxane solution at RT for 30-60 min and dried under vacuum to obtain corresponding hydrochloride salt.

4-((4-(1H-indazol-4-yl)-6-morpholino-1,3,5-triazin-2-yl)oxy)-*N,N'*-dimethylbenzamide hydrochloride salt (26): Yellow solid; Yield: 83%; HPLC purity: 98.2%; mp: 150-155

°C; ^{1}H NMR (300 MHz, DMSO-d_6): δ 8.21 (d, J = 8.1 Hz, 1H), 8.07 (s, 1H), 7.75 (d, J = 8.1 Hz, 1H), 7.54-7.57 (m, 2H), 7.44 (t, J = 7.5 Hz, 1H), 7.36-7.41 (d, J = 10.8 Hz, 2H), 4.01-4.02 (m, 2H), 3.70-3.75 (m, 6H), 3.03 (brs, 6H); ^{13}C NMR (75 MHz, DMSO-d_6): δ 35.4 ($2CH_3$), 43.9, 44.4, 66.2 ($2CH_2$), 115.2, 115.4, 121.5, 122.4, 122.9, 125.9, 128.3, 129.0, 129.5, 134.2, 134.8, 141.0, 153.1, 166.2, 170.0, 171.5, 172.6; ESIMS: 446.2 $[M+1]^+$. HRMS calcd. for $C_{23}H_{24}N_7O_3$: 446.1941, found: 446.1924 $[M+H]^+$.

4-(4-(3-hydroxyphenyl)-6-morpholino-1,3,5-triazin-2-yloxy)-*N,N'*-dimethylbenzamide (1): Off-white solid; Yield: 83%; HPLC purity: 99.7%; mp: 208-215 °C; ^{1}H NMR (300 MHz, DMSO-d_6): δ 9.67 (s, 1H), 7.66-7.70 (m, 2H), 7.50 (d, J = 9.0 Hz, 2H), 7.33 (d, J = 9.0 Hz, 2H), 7.27 (m, 1H), 6.95 (d, J = 9.15 Hz, 1H), 3.94 (s, 2H), 3.62-3.69 (brs, 6H), 2.95-2.99 (m, 6H); ESIMS: 422.2 $[M+1]^+$. HRMS calcd. for $C_{23}H_{24}N_7O_3$: 421.1828, found: 422.1852 $[M+1]^+$.

4-(4-(2-aminopyrimidin-5-yl)-6-morpholino-1,3,5-triazin-2-yloxy)-*N,N'*-dimethylbenzamide hydrochloride salt (2): Off-white solid; Yield: 74%; HPLC purity: 97.5%; mp: 245-255 °C; ^{1}H NMR (300 MHz, DMSO-d_6): δ 8.95 (s, 2H), 7.46-7.50 (m, 4H), 7.30-7.33 (m, 2H), 3.91-3.92 (m, 2H), 3.64-3.66 (m, 2H), 3.60 (s, 4H), 2.94-2.98 (brs, 6H); ^{13}C NMR (75 MHz, MeOD): δ 34.8, 43.2, 43.7, 65.6, 117.2, 121.6, 128.2, 133.3, 152.3, 158.8, 164.9, 165.1, 169.4, 169.7, 170.2; ESIMS: 423.2 $[M+1]^+$. HRMS calcd. for $C_{20}H_{23}N_8O_3$: 422.1893, found: 423.1890 $[M+1]^+$.

4-((4-(6-aminopyridin-3-yl)-6-morpholino-1,3,5-triazin-2-yl)oxy)-*N,N'*-dimethylbenzamide hydrochloride salt (3): White solid; Yield: 81%; mp: 250-259 °C; HPLC purity: 96.4%; ^{1}H NMR (300 MHz, DMSO-d_6): δ 8.71 (s, 1H), 8.49-8.52 (m, 2H), 7.49 (d, J = 8.6 Hz, 2H), 7.32 (d, J = 8.6 Hz, 2H), 7.01 (d, J = 9.2 Hz, 1H), 3.94 (bs, 2H), 3.67 (m, 2H), 3.61 (s, 4H), 2.95-2.98 (brs, 6H); ^{13}C NMR (75 MHz, MeOD): δ 34.7, 43.3, 43.7, 65.7, 113.1, 120.0, 121.4, 128.4, 133.4, 138.4, 141.2, 152.2, 155.5, 165.0, 168.8, 169.4, 170.3; ESIMS: 422.2 $[M+1]^+$. HRMS calcd. for $C_{21}H_{24}N_7O_3$: 421.1941, found: 422.1922 $[M+1]^+$.

4-((4-(6-amino-5-methylpyridin-3-yl)-6-morpholino-1,3,5-triazin-2-yl)oxy)-N,N-dimethylbenzamide (4): Sticky brown oil; Yield: 66%; HPLC purity: 99.0%; ^{1}H NMR (DMSO-d_6, 300 MHz): δ 8.59 (s, 1H), 8.37 (s, 1H), 8.03 (bs, 2H), 7.49 (d, J = 8.7 Hz, 2H), 7.32 (d, J = 8.7 Hz, 2H), 3.95 (bs, 2H), 3.68 (bs, 2H), 3.60 (s, 4H), 2.95-2.99 (m, 6H), 2.21 (s, 3H); ESIMS: 436.3 $[M+1]^+$.

4-(4-(6-amino-4-methylpyridin-3-yl)-6-morpholino-1,3,5-triazin-2-yloxy)-*N,N'*-dimethylbenzamide (5): Light green solid; Yield: 69%; HPLC purity: 92.1%; mp: 118-125 °C; ^{1}H NMR (DMSO-d_6, 300 MHz): δ 8.27-8.30 (m, 1H), 7.50-7.53 (m, 3H), 7.33 (d, J = 8.4 Hz, 2H), 7.25 (d, J = 5.7 Hz, 1H), 3.79 (s, 3H), 3.63-3.67 (m, 6H), 2.95-2.99 (brs, 6H), 2.40 (s, 3H); ESIMS: 436.3 $[M+1]^+$.

4-(4-(6-amino-2-methylpyridin-3-yl)-6-morpholino-1,3,5-triazin-2-yloxy)-*N,N'*-dimethylbenzamide (6): Pale yellow solid; Yield: 69%; HPLC purity: 95.6%; mp: 220-230 °C; ^{1}H NMR (DMSO-d_6, 300 MHz): δ 7.77-7.93 (m, 2H), 7.49-7.58 (m, 3H), 7.32 (d, J = 8.5 Hz, 2H), 7.12-7.15 (m, 1H), 3.76 (s, 2H), 3.66 (s, 6H), 2.94-2.99 (brs, 6H), 2.40 (s, 3H); ESIMS: 436.2 $[M+1]^+$.

4-(4-(1H-indol-4-yl)-6-morpholino-1,3,5-triazin-2-yloxy)-*N,N'*-dimethylbenzamide (7): Off-white solid; Yield 64%; HPLC purity: 87.3%; mp: 120-130 °C; ^{1}H NMR (300 MHz, DMSO-d_6): δ 11.32-11.34 (m, 1H), 8.10-8.13 (m, 1H), 7.58-7.61 (m, 1H), 7.52-7.55 (m, 2H), 7.35-7.37 (m, 2H), 7.28-7.32 (m, 1H), 7.13-7.22 (m, 1H), 6.81-6.83 (m, 1H), 3.99 (s, 2H), 3.69-3.73 (m, 6H), 3.01 (s, 6H); ESIMS: 445.1 $[M+1]^+$.

***N,N'*-dimethyl-4-((4-morpholino-6-(1H-pyrrolo[2,3-c]pyridin-4-yl)-1,3,5-triazin-2-yl)oxy)benzamide hydrochloride salt (8) :** Off-white solid; Yield: 66 %; HPLC purity: 97.8%; mp: 206-215 °C; ^{1}H NMR (300 MHz, DMSO-d_6): δ 12.14 (s, 1H), 9.09 (d, J = 1.74 Hz, 1H), 8.85 (d, J = 1.62 Hz, 1H), 7.58-7.59 (m, 1H), 7.51 (d, J = 8.4 Hz, 2H), 7.35 (d, J = 8.4 Hz, 2H), 6.60-6.61 (m, 1H), 3.99 (bs, 2H), 3.63-3.70 (m, 6H), 2.97-2.99 (brs, 6H); ESIMS: 446.5 $[M+1]^+$.HRMS calcd. for $C_{23}H_{24}N_7O_3$: 445.1941, found: 446.1919 $[M+1]^+$.

4-(4-(1H-benzo[d][1,2,3]triazol-4-yl)-6-morpholino-1,3,5-triazin-2-yloxy)-*N,N'*-dimethylbenzamide (9): Off-white solid; Yield 55%; HPLC purity: 86.7%; mp: 142-150 °C; ^{1}H NMR (300 MHz, DMSO-d_6): δ 8.18-8.21 (m, 1H), 7.87-7.90 (m, 1H), 7.36-7.56 (m, 5H), 3.79-3.85 (m, 2H), 3.60-3.66 (m, 6H), 3.59 (m, 1H), 2.99-3.01 (brs, 6H); ESIMS: 447.5 $[M+1]^+$.

4-((4-(2-aminothiazol-5-yl)-6-morpholino-1,3,5-triazin-2-yl)oxy)-*N,N'*-dimethylbenzamide hydrochloride salt (10): Off-white solid. Yield: 85%; mp: 276-283 °C; HPLC purity: 99.6%; ^{1}H NMR (300 MHz, DMSO-d_6): δ 8.39 (bs, 2H), 7.94 (s, 1H), 7.46 (d, J = 8.4 Hz, 2H), 7.28 (d, J = 8.4 Hz, 2H), 3.80 (s, 2H), 3.57-3.64 (m, 6H), 2.93-2.98 (brs, 6H); ^{13}C NMR (75 MHz, MeOD): δ 34.3, 43.5, 44.0, 65.9, 66.0, 121.6, 123.4, 128.2, 129.7, 133.2, 153.0, 165.1, 166.2, 170.4, 171.3, 171.5; ESI-MS: 428.2 $[M+1]^+$. HRMS calcd. for $C_{19}H_{22}N_7O_3S$: 427.1505, found: 428.1488 $[M+1]^+$.

4-((4-(2-amino-4-methylthiazol-5-yl)-6-morpholino-1,3,5-triazin-2-yl)oxy)-*N,N'*-dimethylbenzamide hydrochloride salt (11): White solid; Yield 70%; HPLC purity: 95.8%; mp: 225-232 °C; ^{1}H NMR (300 MHz, DMSO-d_6): δ 7.65 (s, 2H), 7.44-7.47 (m, 2H), 7.25-7.28 (m, 2H), 3.75 (m, 2H), 3.61-3.65 (m, 6H), 2.92-2.98 (brs, 6H), 2.30 (s, 3H); ESIMS: 442.3 $[M+1]^+$.

4-((4-(2-amino-1H-imidazol-5-yl)-6-morpholino-1,3,5-triazin-2-yl)oxy)-*N,N'*-dimethylbenzamide hydrochloride salt (12): Sticky yellow solid; Yield 62%; HPLC purity: 97.9%; ^{1}H NMR (300 MHz, DMSO-d_6): δ 10.97 (bs, 1H), 7.44-7.47 (m, 2H), 7.25-7.32 (m, 2H), 5.81 (m, 2H), 3.87 (s, 2H), 3.52-3.64 (m, 6H), 2.94-2.98 (brs, 6H); ESIMS: 411.7 $[M+1]^+$.

Gram scale synthesis of 4-((4-(2-aminothiazol-5-yl)-6-morpholino-1,3,5-triazin-2-yl)oxy)-*N,N'*-dimethylbenzamide hydrochloride salt (10): To a mixture of compound **13** (10 g, 25.0 mmol) in anhydrous DMF (20 mL) was added *tert*-butyl 5-(tributylstannyl)thiazol-2-ylcarbamate **14** (14.7 g, 30.0 mmol). The resulting mixture was degassed (repeated nitrogen and vacuum cycles) for 15 min followed by

addition of $Pd(PPh_3)_4$ (2.85 g, 2.50 mmol) under inert atmosphere. The reaction mixture was heated to reflux under inert atmosphere for 4 h. Progress of the reaction was monitored by TLC. After consumption of starting material, the excess of DMF was removed under reduced pressure and reaction mixture was extracted with DCM (3 x 500 mL). The organic layer was washed with brine, seperated and dried over anhydrous Na_2SO_4, filtered and evaporated under reduced pressure to obtain viscous dark brown material which was further purified by silica gel chromatography (Eluent: 0-35% EtOAC/ Hexane mixture) to obtain product as light yellow sticky solid, *i.e., tert*-butyl (5-(4-(4-(dimethylcarbamoyl)phenoxy)-6-morpholino-1,3,5-triazin-2-yl)thiazol-2-yl)carbamate, [*N*-Boc protected **10** (9.43 g, 65%). ESIMS: 528.1 $[M+1]^+$. This obtained product (9.4 g, 17.8 mmol) was dissolved in anhydrous DCM (100 mL). To this mixture, 4N HCl in dioxane (100 mL) was added drop wise at 0 °C and resulting mixture was then stirred at RT for 6 h. After completion (TLC), reaction mixture was evaporated under vacuum and residue so obtained was treated with diethyl ether and dried under vacuum to obtain compound **10** as off-white solid. Yield: (7.02g, 85%).

PI3K*α* enzyme assays: Kinase activity was measured in a homogeneous assay in low-binding Corning 384 well white plates. Detection was performed by HTRF using ADP detection mixture comprising of ADP HiLyte 647 tracer bound to an ADP2 antibody-Tb conjugate. (Transcreener® ADP2 TR-FRET Red Assay, Bell Brook Labs, Madison, WI) 2.5 µL of compound ranging from 10 µM - 0.001 µM were added to a 384 well plate. 2.5 µL of diluted PI3K alpha 150 ng/mL (Invitrogen Life Sciences) in a reaction buffer consisting of 50mM HEPES, pH 7.4, 3mM $MgCl_2$, 2 mM DTT, 0.05% CHAPS, 50 mM NaCl, and 1mM EGTA was added and the plates were incubated for 15 min with shaking. The reaction was initiated by addition of PIP2 & ATP (50 µM PIP2 & 1 µM ATP in final assay). The samples were incubated for 60 minutes. 10 µL of ADP Detection mix was added and incubated for 1 h. The plate was read in an Envision Multilabel Plate Reader. Fluorescence was measured at 665 nm & 615 nm. The ratio between the signal at 665 and 615 nm was calculated. The percentage of inhibition was calculated and plotted against the concentration of inhibitor. IC_{50} was calculated using Graph Pad prism Non-linear regression fit (Log inhibitor *vs* variable slope using four parameters).

mTOR Assay: Compounds were evaluated for mTOR activity using invitro kinase assay. mTOR activity is measured in vitro by determining the level of phosphorylation of the protein substrate 4EBP-1. The phosphorylation of GFP-4E-BP1 at threonine residue is recognized by Ab Tb-Anti-p4EBP1, which results in time resolved fluorescence energy transfer (TR-FRET) between GFP and Terbium in the Ab-Protein complex. Recombinant mTOR (FRAP1), Kinase reaction buffer, GFP-4E-BP1 and LanthaScreen Tb-anti-4E-BP1 (pThr46), TR FRET dilution buffer, Kinase Quench Buffer were obtained from Invitrogen. Kinase reactions were performed in 10 µL volume in 384 well plates. Serially diluted compounds (10 µM-0.0005 µM) prepared in DMSO were incubated with mTOR in the assay buffer for 15 min. Reaction was initiated by the addition of substrate (GFP-4E-BP1) and ATP at final conc. of 400 nM and 8 µM ATP in the reaction respectively. Kinase reaction was allowed to proceed for 1 h at RT before a 10 µL preparation of kinase quench buffer and Tb–labeled Antibody in TR-FRET dilution buffer was added. Plate was incubated at RT for 1 h. FRET signal was read in Envision Multilabel Reader. TR FRET Ratio (Fluorescence 520 nm/Fluorescence 486 nm) was plotted against the concentration of inhibitor and data was fit to Non Linear Regression curve fit (sigmoidal dose response curve with variable slope-four parameters) using Graph pad prism 5.

***In vitro* Anti-proliferative activity by MTT assay:**

A2780: A2780 cells (human ovarian cancer) were cultured in DMEM (Sigma) supplemented with 10% FBS, L-glutamine and antibiotics. Cells were plated in the same medium at the density of 10000 cells/ well into 96 well tissue culture plates and allowed to adhere overnight. Cells were treated with compounds in the concentration range 20 µM - 0.001 µM for 48 h. A 10 µL solution of MTT (3-(4,5-dimethythiazol-2-yl)-2,5-diphenyl tetrazolium bromide) 5 mg/ mL in PBS was added to the wells. The plates were incubated for 4 h. The plates were then centrifuged at 1000 rpm for 5 min, supernatant was removed and 100 µL DMSO was added and mixed on shaker for 30 min. Absorbance was measured at 550 nm in an Envision Multilabel Plate Reader (Perkin Elmer). The percentage of inhibition was calculated and a dose response curve was plotted using Graph pad Prism with a non-linear regression fit (Log inhibitor *vs.* variable slope, four parameters).

PC3: PC3 human prostate cancer cells (American Type Culture Collection, Manassas, VA) were cultured in RPMI 1640 (Invitrogen, Carlsbad, CA) supplemented with 10% fetal bovine serum and 1% penicillin and streptomycin in a 5% CO_2 atmosphere at 37 °C. Cells were plated in the same medium at the density of 10000 cells/ well into 96 well tissue culture plates. Cells were treated with compounds in the concentration range 20 µM - 0.001 µM for 48 h. A 10 µL solution of MTT (3-(4,5-dimethythiazol-2-yl)-2,5-diphenyl tetrazolium bromide) 5 mg/ ml in PBS was added to the wells. The plates were incubated for 4 h. The plates were then centrifuged at 1000 rpm for 5 min, supernatant was removed and 100 µL DMSO was added and mixed on shaker for 30 min. Absorbance was measured at 550 nm in an Envision Multilabel Plate Reader (Perkin Elmer). The percentage of inhibition was calculated and a dose response curve was plotted using Graph pad Prism with a non-linear regression fit (Log inhibitor *vs*. variable slope, four parameters).

SKOV3: SK-OV-3 human ovarian cells was grown in McCoy's 5a medium supplemented with 10% fetal bovine serum, 100 U/mL penicillin and 100 µg/mL streptomycin at 37ºC in an atmosphere of 5% CO_2 in air. Cells were plated in the same medium at the density of 10000 cells/ well into 96 well tissue culture plates. Cells were treated with compounds in the concentration range 20 µM - 0.001 µM for 48 h. A 10 µL solution of MTT (3-(4,5-dimethythiazol-2-yl)-2,5-diphenyl tetrazolium bromide) 5 mg/mL in PBS was added to the wells. The plates were incubated for 4 h. The plates were then centrifuged at 1000 rpm for 5 min, supernatant was removed and 100 µL DMSO was added and mixed on shaker for 30 min. Absorbance was measured at 550 nm in an Envision Multilabel Plate Reader (Perkin Elmer). The percentage of inhibition was calculated and a dose response curve was

plotted using Graph pad Prism with a non-linear regression fit (Log inhibitor *vs.* variable slope, four parameters).

Microsomal stability assay: 10 µM Compound was incubated with 0.5 mg/mL liver microsomes (MLM, DLM, HLM purchased from BD Gentest). NADPH was maintained at 1 mM in the final assay in 700 µL reaction volume. The reaction was evaluated at 0, 15, 30, 60 & 120 min and was terminated by the addition of acetonitrile. Samples were centrifuged for 10 min at 10000 rpm and supernatant analyzed using HPLC. Percentage parent remaining was calculated considering percent parent area at 0 min as 100%.

Experimental details for pharmacokinetic evaluations of the compounds: Female Swiss mice, (3 animals per group) after overnight fasting were dosed orally (*via* gavage) with test compound in 0.5% CMC/0.5% Tween 80 (10 mL/kg) at dose levels of 1, 3, 10 mg/kg. Blood was collected by serial bleeding at 0.16 h, 0.5 h, 1 h, 2 h, 4 h, 6 h, 8 h, respectively in heparinized tubes. Blood samples were centrifuged at 10,000 rpm for 5 min at 4 °C to obtain the plasma, which were aspirated into separate labeled tubes and stored at -80 °C. 400 ng/mL of Verapmil in acetonitrile was used as the drug extraction solvent for extracting drug from plasma. Extraction solvent was added to plasma was vortexed and shaken using an auto-shaker for 10 min, centrifuged at 10000 rpm for 10 min at 40 °C. Supernatant was retained for analysis. Acetonitrile and plasma calibration curves were generated and percentage of drug recovery from plasma determined by a quantitative analysis using LCMS. Quantitative analysis was done by liquid chromatography tandem mass spectrometer (API3000 LC-MS/MS). C_{max}, T_{max}, AUC and $t_{1/2}$ were calculated using Graph Pad PRISM version 5.04.

Experimental detail for hERG activity analysis: HERG-Lite monitors the expression of hERG (human ether-à-go-go)-related gene at the cell surface in two different stable mammalian cell lines. One cell line acts as a biosensor for drugs that inhibit hERG trafficking, while the other predicts hERG blockers based on their ability to act as pharmacological chaperones. The *in vitro* effects of the selected compounds were evaluated for effecting changes in relative surface expression (RSE) of the hERG potassium channel. Trafficking inhibition was assessed by monitoring surface expression of the wild-type (WT) channel, while channel block was predicted based on the rescue of surface expression of a hERG single mutant (SM). Compounds were tested at 1, 10, 30 µM concentrations. Geldanamycin at 1 µM was used as inhibitor of hERG trafficking and Astemizole was used as a standard hERG binder.

Kinase biochemical assay for 23 kinases by microfluidic mobility shift detection: SPR519 was tested against 23 kinases at a single test concentration of 1 µM in duplicate wells. Test compound was diluted in DMSO to 100x assay concentration and then further diluted in assay buffer. The final concentration of DMSO in all assays was kept at 1%. Reference compounds, Staurosporine and Wortmannin, were tested in 8-point IC_{50} format using 3-fold dilution steps. Test compound, enzyme, fluorescently labeled substrate, and cofactors (ATP and Mg^{2+}) were combined in a well of a microtiter plate and incubated typically for 3 h at 25 ºC. ATP was used at 1 x Km concentration, while typical concentrations of the peptide substrate and the kinase are 1 µM and 1 nM, respectively. At the end of the incubation, the reaction was quenched by the addition of an EDTA-containing buffer. Substrate and product (*i.e.,* phosphorylated substrate) were separated electrophoretically using the microfluidic-based LabChip 3000 Drug Discovery System from Caliper Life Sciences and both were quantitated by fluorescence intensity.

Cyp P450 inhibition assay: The *in vitro* inhibition of cytochrome P450 (CYP) 2C9, 2C19, 2D6, and 3A4 isozymes by **SPR519** was evaluated in human liver microsomes. The inhibition of each isozyme by the test items was monitored by following the production of a selected metabolite of an FDA-recommended probe substrate of the respective isozyme using HPLC and LC-MS/MS technique. For each isozyme, the incubations were performed in duplicate in a 96-well plate. Microsomes-buffer-substrate mixtures (MBS mix) were prepared by pre-mixing appropriate volumes of buffer, human liver microsomes and CYP-specific probe substrates. This MBS mixture (179 µL) was transferred to a 96-well plate and 1 µL of inhibitor stock solutions were spiked into it such that the final target inhibitor concentrations were achieved. The plate was incubated at 37 °C for 5 min following which the reaction was initiated by the addition of 20 µL of 10 mM NADPH. The reaction plate was incubated at 37 °C for a pre-determined time and subsequently it was quenched with 200 µL of respective stop solutions. The formation of each substrate metabolite was monitored using HPLC and LCMS. The effect of increasing the concentration of test items on the production of the metabolite was evaluated, and the concentration of inhibitor required for a 50% reduction in the measured enzyme activity was determined.

Experimental details for multiple day dose tolerance study: Female swiss mice were dosed 10mpk for 5 days BID and 30mpk for 12 days BID to evaluate drug related toxicity in mice on repeat dosing. 3 Female Swiss mice, were administered 10mpk of **SPR519** formulated in CMC 0.5% and Tween 80, by oral gavage twice a day (BID) for a period of 5 days. 2 mice were kept as control. Parameters like body weight, body temperature, body coat, feed intake and general activities were monitored on a daily basis. 4 Female Swiss mice, were administered 30mpk of test compound (SPR519) formulated in CMC 0.5% and Tween 80, by oral gavage twice a day (BID) for a period of 12 days. 2 mice were kept as control. Parameters like body weight, body temperature, body coat, feed intake and general activities were monitored on a daily basis.

Experimental details for tissue distribution study of SPR519 after repeat dosing: Three female Swiss mice, were administered 30mpk of **SPR519** formulated in CMC 0.5% and Tween 80, by oral gavage twice a day (BID) for a period of 5 days. Two mice were kept as control. Parameters like body weight, body temperature, body coat, feed intake and general activities were monitored on a daily basis. On the last day, mice were anesthetized by isofluorane and euthanized via cardiac puncture. Liver, brain, uterus and kidneys were removed from each animal by gross dissection. After flushing with saline, tissues were stored. Tissues were rinsed gently, but thoroughly with water to remove remaining traces of blood before storage. Dissecting instruments were also washed between tissue procurements to avoid cross-contamination.

Aqueous homogenates of the tissue were prepared. Extraction solvent was added to tissues vortexed and shaken using an auto-shaker for 10 min, centrifuged at 10000 rpm for 10 min at 40 °C. Supernatant was retained for analysis. Acetonitrile and plasma calibration curves were generated and percentage of drug recovery from tissue was determined by a quantitative analysis using LCMS. Tissue levels of the drug were evaluated by liquid chromatography tandem mass spectrometer (API3000 LC-MS/MS).

Experimental detail for *in vivo* efficacy study: The xenograft was generated by subcutaneous injection of HCT116 and SKOV3 in CD1 nude mice. Animals were randomized in 5 groups (Vehicle control, Standard Drug, test Compound in multiple doses) and treatment was started when average tumor size was 120-130 mm^3. The body weight was checked prior to dosing or alternate day as required. The size of the tumor was measured every alternate day. The tumor size was measured by taking longest length and shortest width of the tumor with digital caliper. The tumor volume was calculated with the formula ($width^2$ x length)/2. On the last day of study, CO_2 overdosing was done to euthanize the animals to complete the experiment. Tumor isolation was done and snap frozen in liquid nitrogen followed by storage at -80 °C for further studies. Complete liver and lung tissue was isolated and snap frozen.

AUTHOR INFORMATION

Corresponding Authors

*†dinesh.mahajan@thsti.res.in; chemidinesh@gmail.com
*dugar.s@sphaerapharma.com

Present Addresses

† Principal Scientist-II, Translational Health Science and Technology Institute (THSTI), NCR Biotech Cluster, Faridabad, INDIA 121001.

Notes

All experimental *in vivo* work related to animals were performed after due approvals and performed in accordance with institutional guidelines as defined by Institutional Animal ethics committee.

The authors declare the following competing financial interest (s): All the authors are current or past employee of Sphaera Pharma. SD is shareholder of Sphaera Pharma.

ACKNOWLEDGMENT

Authors wish to acknowledge Dr Sandip Bharate -IIIM Jammu for kind help on HRMS experiments and Mr. Ashish Dugar at Sphaera Pharma for his untiring efforts for extraction of old data files.

ASSOCIATED CONTENT

Supporting Information

Images of NMR (^1H and ^{13}C) as well as MS/HRMS spectra, HPLC chromatograms and molecular formula strings for all new compounds described in this paper are available as supporting information at http://pubs.acs.org.

ABBREVIATIONS

PI3K, phosphoinositide 3-kinase; Akt, protein kinase B; mTOR, mechanistic or mammalian target of rapamycin; S6K, S6 kinase; mTOR, mammalian target of rapamycin; TR-FRET, time-resolved Forster resonance energy transfer; DIPEA, N,N-diisopropylethylamine; DMF, Dimethylformamide; PK, pharmacokinetic; AUC, Area Under Curve; DTT, Dithiothreitol; CHAPS, 3-[(3-Cholamidopropyl)dimethylammonio]-1-propanesulfonate; EGTA, Ethylene-bis(oxyethylenenitrilo)tetraacetic acid

REFERENCES

1. Cantley, L. C. The phosphoinositide 3-kinase pathway. *Science* **2002**, *296*, 1655−1657.
2. Toker, A.; Cantley, L. C. Signalling through the lipid products of phosphoinositide-3-OH kinase. *Nature* **1997**, *387*, 673−676.
3. Fruman, D. A.; Rommel, C. PI3K and cancer: Lessons, challenges and opportunities. *Nat. Rev. Drug Discov.* **2014**, *13*, 140−156.
4. Jean, S.; Kiger, A. A. Classes of phosphoinositide 3-kinases at a glance. *J. Cell Sci.* **2014** *127*, 923–928.
5. Thorpe, L. M.; Yuzugullu, H.; Zhao, J. J. PI3K in cancer: Divergent roles of isoforms, modes of activation and therapeutic targeting. *Nat. Rev. Cancer* **2015**, *15*, 7−24.
6. Janku, F. Phosphoinositide 3-kinase (PI3K) pathway inhibitors in solid tumors: From laboratory to patients. *Cancer Treat. Rev.* **2017**, *59*, 93−101.
7. Janku, F.; Yap, T. A.; Bernstam, M. F. Targeting the PI3K pathway in cancer: Are we making headway? *Nat. Rev. Clin. Oncol.* **2018**, *15*, 273-291.
8. Enrique Rozengurt, E.; Soares, H.P.; Smith, J. S. Suppression of feedback loops mediated by PI3K/mTOR induces multiple over-activation of compensatory pathways: An unintended consequence leading to drug resistance. *Mol. Cancer Ther.* **2014**, *13*, 2477–2488.
9. Liu Y. N.; Wan R. Z.; Liu Z. P. Recent developments of small molecule PI3K/mTOR dual inhibitors. *Mini Rev. Med. Chem.* **2013**, *13*, 2047−2059.
10. Garces, A.E.; Stocks, M.J. Class I PI3K clinical candidates and recent inhibitor design strategies: A medicinal chemistry perspective. *J. Med. Chem.*, **2019**, *62*, 4815-4850.
11. Yaguchi, S.I.; Fukui, Y.; Koshimizu, I.; Yoshimi, H.; Matsuno, T.; Gouda, H. ; Hirono, S.; Yamazaki, K.; Yamori, T. Antitumor activity of ZSTK474, a new phosphatidylinositol 3-kinase inhibitor. *J. Natl. Cancer Inst.* **2006**, *98*, 545-556.
12. Venkatesan, A.M.; Dehnhardt, C.; Santos, E.D.; Chen, Z.; Santos, O.D.; Kaloustian, S.A.; Khafizova, G.; Brooijmans, N.; Mallon, R.; Hollander, I.; Feldberg, L.; Lucas, J.; Yu, K.; Gibbons, J.; Abraham, R.T.; Chaudhary, I.; Mansour, T.S. Bis(morpholino-1,3,5-triazine) derivatives: Potent adenosine 50-triphosphate competitive phosphatidylinositol-3-kinase/mammalian target of rapamycin inhibitors: Discovery of compound 26 (PKI-587), a highly efficacious dual inhibitor. *J. Med. Chem.* **2010**, *53*, 2636–2645.
13. Beaufils, F.; Cmiljanovic, N.; Cmiljanovic, V.; Bohnacker, T.; Anna Melone, A.; Marone, R.; Jackson, E.; Zhang, X.; Sele, A.; Borsari, C.; Mestan, J.; Hebeisen, P.; Hillmann, P.; Giese, B.; Zvelebil, M.; Fabbro, D.; Williams, R.L.; Rageot, D.; Wymann, M.P. 5‐(4,6-Dimorpholino-1,3,5-triazin-2-yl)-4-(trifluoromethyl)pyridin-2-amine (PQR309), a potent, brain-penetrant, orally bioavailable, Pan-Class I PI3K/mTOR inhibitor as clinical candidate in oncology. *J. Med. Chem.* **2017**, *60*, 7524−7538.
14. Borsari, C.; Rageot, D.; Beaufils, F.; Bohnacker, T.; Keles, E.; Buslov, I.; Melone, A.; Sele, A.M.; Hebeisen, P.; Fabbro, D.; Hillmann, P.; Wymann, M.P. Preclinical

development of PQR514, a highly potent PI3K inhibitor bearing difluoromethyl−pyrimidine moiety. *ACS Med. Chem. Lett.* **2019**, *10*, 1473−1479.

15. Rageot, D.; Bohnacker, T.; Keles, E.; McPhail, J.A.; Hoffmann, R.M.; Melone, A.; Borsari,C.; Sriramaratnam, R.; Sele, M.A.; Beaufils, F.; Hebeisen, P.; Fabbro, D.; Hillmann, P.; Burke, J.E.; Wymann, M.P. (S) -4-(Difluoromethyl)-5-(4-(3-methylmorpholino)-6-morpholino-1,3,5-triazin-2-yl)pyridin-2-amine (PQR530), a potent, orally bioavailable, and brain-penetrable dual inhibitor of class I PI3K and mTOR Kinase. *J. Med. Chem*. **2019**, *62*, 6241−6261.
16. Andrs, M.; Korabecny, J.; Jun, D.; Hodny, Z.; Bartek, J.; Kuca, K. Phosphatidylinositol 3 -kinase (PI3K) and phosphatidylinositol 3 -kinase-related kinase (PIKK) inhibitors: Importance of the morpholine ring. *J. Med. Chem*. **2015**, *58*, 41−71.
17. Dugar, S.; Hollinger, F. P.; Mahajan, D.; Sen, S.; Kuila, B.; Arora R.; Pawar, Y.; Shinde, V.; Rahinj, M.; Kapoor, K. K.; Bhumkar, R.; Rai, S.; Kulkarni, R. Discovery of novel and orally bioavailable inhibitors of PI3Kinase based on indazole substituted morpholino-triazines. *ACS Med. Chem. Lett.* **2015**, *6*, 1190−1194.
18. Dugar, S.; Hollinger, F. P.; Kuila, B.; Arora, R.; Sen, S.; Mahajan, D. Synthesis and evaluation of pyrrolotriazine based molecules as PI3Kinase inhibitors. *Bioorg. Med. Chem. Lett.* **2015**, *25*, 3142−3146.
19. Folkes, A. J.; Ahmadi, K.; Alderton, W. K.; Alix, S.; Baker, S. J.; Box, G.; Chuckowree, I. S.; Clarke, P. A.; Depledge, P.; Eccles, S. A.; Friedman, L. S.; Hayes, A.; Hancox, T. C.; Kugendradas, A.; Lensun, L.; Moore, P.; Olivero, A. G.; Pang, J.; Patel, S.; Pergl-Wilson, G. H.; Raynaud, F. I.; Robson, A.; Saghir, N.; Salphati, L.; Sohal, S.; Ultsch, M. H.; Valenti, M.; allweber, H. J. A.; Wan, N. C.; Wiesmann, C.; Workman, P.; Zhyvoloup, A.; Zvelebil, M. J.; Shuttleworth, S. J. The identification of 2-(1*H* -Indazol-4-yl)-6-(4-methanesulfonyl-piperazin-1-ylmethyl)-4-morpholin-4-yl-thieno[3,2-*d*]pyrimidine (GDC-0941) as a potent, selective, orally bioavailable inhibitor of class I PI3 kinase for the treatment of cancer†. *J. Med. Chem*. **2008**, *51*, 5522−5532.
20. Berndt, A.; Miller, S.; Williams, O.; Le, D. D.; Houseman, B. T.; Pacold, J. I.; Gorrec, F.; Hon, W.-C.; Ren, P.; Liu, Y.; Rommel, C.; Gaillard, P.; Rückle, T.; Schwarz, M. K.; Shokat, K. M.; Shaw, J. P.; Williams, R. L. The P110δ structure: Mechanisms for selectivity and potency of new PI(3)K inhibitors. *Nat. Chem. Biol*. **2010**, *6*, 117−124.
21. Dugar, S.; Mahajan, D.; Hollinger, F. P.; Sharma, A; Kuila, B. Novel triazine compounds. US 2015/0197515 A1.

Graphical Abstract

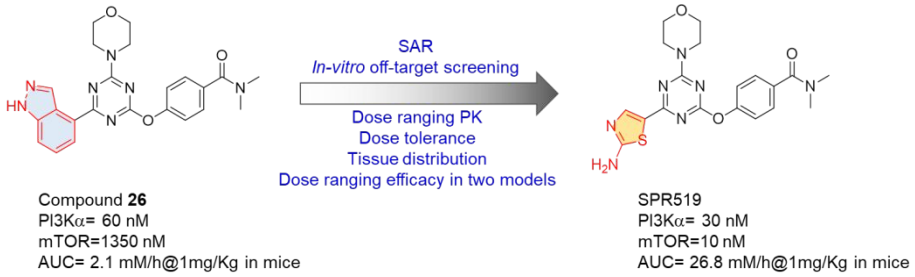

Compound **26**
PI3Kα= 60 nM
mTOR=1350 nM
AUC= 2.1 mM/h@1mg/Kg in mice

SPR519
PI3Kα= 30 nM
mTOR=10 nM
AUC= 26.8 mM/h@1mg/Kg in mice